Cellular and metabolic characteristics of pre-leukemic hematopoietic progenitors with GATA2 haploinsufficiency

Avigail Rein,[1,2,3] Ifat Geron,[1,2,3,4] Eitan Kugler,[1,2,3] Hila Fishman,[1,2,3] Eyal Gottlieb,[5] Ifat Abramovich,[5] Amir Giladi,[6] Ido Amit,[6] Roger Mulet-Lazaro,[7] Ruud Delwel,[7,8] Stefan Gröschel,[7,9,10] Smadar Levin-Zaidman,[11] Nili Dezorella,[11] Vered Holdengreber,[12] Tata Nageswara Rao,[13] Joanne Yacobovich,[2] Orna Steinberg-Shemer,[2,4] Qiu-Hua Huang,[14] Yun Tan,[14,15] Sai-Juan Chen,[14,15] Shai Izraeli[1,2,3,4] and Yehudit Birger[1,2,3,4]

[1]Department of Human Molecular Genetics and Biochemistry, Sackler Medical School, Tel Aviv University, Tel Aviv, Israel; [2]The Rina Zaizov Division of Pediatric Hematology-Oncology, Schneider Children's Medical Center, Petah Tikva, Israel; [3]Functional Genomics and Childhood Leukaemia Research, Sheba Medical Centre, Tel-Hashomer, Israel; [4]Felsenstein Medical Research Center, Sackler School of Medicine, Tel Aviv University, Petah Tikva, Israel; [5]Technion Integrated Cancer Center, Faculty of Medicine, Technion Israel Institute of Technology, Haifa, Israel; [6]Department of Immunology, Weizmann Institute of Science, Rehovot, Israel; [7]Department of Hematology, Erasmus University Medical Center, Rotterdam, The Netherlands; [8]Oncode Institute, Erasmus University Medical Center, Rotterdam, The Netherlands; [9]Molecular Leukemogenesis, Deutsches Krebsforschungszentrum, Heidelberg, Germany; [10]Department of Internal Medicine V, Heidelberg University Hospital, Heidelberg, Germany; [11]Electron Microscopy Unit, Weizmann Institute of Science, Rehovot, Israel; [12]Electron Microscopy Unit, IDRFU, Faculty of Life Sciences, Tel Aviv University, Israel; [13]Stem Cells and Leukemia Laboratory, University Clinic of Hematology and Central Hematology, Department of Biomedical Research (DBMR), Inselspital Bern, University of Bern, Bern, Switzerland; [14]State Key Laboratory of Medical Genomics, Shanghai Institute of Hematology, Rui Jin Hospital Shanghai, China and [15]Jiao Tong University School of Medicine, Shanghai, China

Correspondence:
S. Izraeli
sizraeli@gmail.com

Y. Birger
Yehudit.Birger@gmail.com

Received: June 21, 2021.
Accepted: December 1, 2022.
Early view: December 7, 2022.

https://doi.org/10.3324/haematol.2022.279437

©2023 Ferrata Storti Foundation
Published under a CC BY-NC license

Abstract

Mono-allelic germline disruptions of the transcription factor GATA2 result in a propensity for developing myelodysplastic syndrome (MDS) and acute myeloid leukemia (AML), affecting more than 85% of carriers. How a partial loss of GATA2 functionality enables leukemic transformation years later is unclear. This question has remained unsolved mainly due to the lack of informative models, as *Gata2* heterozygote mice do not develop hematologic malignancies. Here we show that two different germline *Gata2* mutations (Tg*Erg/Gata2*^{het} and Tg*Erg/Gata2*^{L359V}) accelerate AML in mice expressing the human hematopoietic stem cell regulator ERG. Analysis of *Erg/Gata2*^{het} fetal liver and bone marrow-derived hematopoietic cells revealed a distinct pre-leukemic phenotype. This was characterized by enhanced transition from stem to progenitor state, increased proliferation, and a striking mitochondrial phenotype, consisting of highly expressed oxidative-phosphorylation-related gene sets, elevated oxygen consumption rates, and notably, markedly distorted mitochondrial morphology. Importantly, the same mitochondrial gene-expression signature was observed in human AML harboring *GATA2* aberrations. Similar to the observations in mice, non-leukemic bone marrows from children with germline *GATA2* mutation demonstrated marked mitochondrial abnormalities. Thus, we observed the tumor suppressive effects of GATA2 in two germline *Gata2* genetic mouse models. As oncogenic mutations often accumulate with age, GATA2 deficiency-mediated priming of hematopoietic cells for oncogenic transformation may explain the earlier occurrence of MDS/AML in patients with *GATA2* germline mutation. The mitochondrial phenotype is a potential therapeutic opportunity for the prevention of leukemic transformation in these patients.

Introduction

The hematopoietic transcriptional machinery is a network of highly tuned feedback circuits. Dysfunction of a pivotal regulator might, therefore, hinder its entire performance. GATA2 is a cardinal hematopoietic transcription factor critical for initiation of fetal hematopoiesis and for maintaining the hematopoietic stem cell pool throughout life by restricting stem cell differentiation.[1-3]

Abnormal regulation of GATA2 expression and somatic mutations in *GATA2* have been associated with both tumor promotion and tumor inhibition.[4,5] Yet germline heterozygous mutations in *GATA2*, most of which are loss-of-function, are uniformly associated with increased

risk of myeloid malignancies.[6,7] *GATA2* germline haploinsufficiency syndrome is a multisystem disorder with a highly variable clinical presentation.[8,9] The most common and most serious consequence of the disorder is the propensity to develop myelodysplastic syndrome (MDS) or acute myeloid leukemia (AML), which affect more than 80% of diagnosed carriers before the age of 40.[8,10,11] More than 150 unique mutations have been associated with *GATA2* haploinsufficiency,[8,11,12] including missense-substitutions, nonsense-truncations, and small indels. Additional secondary oncogenic changes often contribute to leukemic transformation. Hence, the optimal timing for bone marrow (BM) transplantation, currently the sole therapeutic strategy for GATA2 deficiency, is unclear. There is, therefore, an unmet need to decipher cellular events that precede malignancy in carriers of germline *GATA2* mutations.

One of the problems is the scarsity of pre-clinical models. While total ablation of murine *Gata2* confers embryonic lethality,[2,13] heterozygous mice display only a mild phenotype and do not develop MDS or leukemia.[13,14] As hematopoietic malignancies in patients with germline *GATA2* abnormalities are characterized by additional somatic oncogenic mutations, it is reasonable to hypothesize that the tumor suppressive effect of *Gata2* deficiency will be revealed in mice expressing a hematopoietic oncogene. Interestingly, germline *Gata2* haploinsufficiency delayed the occurrence of leukemia in mice carrying *CbfbMYH11* fusion,[15] while it accelerated leukemogenesis in mice expressing *Evi1*[16] or loss of *C/Ebp* alpha,[17] respectively. These later studies focused on a detailed analysis of the mouse leukemias but not on the pre-leukemic phenotype.

Here we report a detailed analysis of the impact of Gata2 deficiency on hematopoietic stem and progenitor cells (HSPC) at the pre-leukemic phase. We examined the hypothesis that the implication of dysfunctional Gata2 in mice would be maximized on expression of a stem cell oncogene. ERG, a hematopoietic Ets transcription factor that is an up-stream regulator of GATA2,[18] is a potent regulator of normal and leukemic stem cells.[19,20] ERG has recently been shown to be the main driver of AML caused by haploinsufficiency of *GATA2* with increased expression of *EVI*-1.[21] In line with this, we traced the trajectories of HSPC with heterozygous germline *Gata2* deficiency from gestation to leukemia in *ERG* transgenic mice. We show that the loss of *Gata2* caused early expansion of proliferative hematopoietic progenitor cells that had already been detected at the fetal liver stage, long before overt leukemic transformation. We also observed that haploinsufficiency of *Gata2* induced a mitochondrial phenotype in these pre-leukemic cells. Significantly, this was confirmed in children with germline *GATA2* haploinsufficiency and in human AML with *GATA2* mutations.

Methods

Mice handling

Double transgenic mice were generated by crossing Tg*ERG*[18] mice (from two different Tg*ERG* F_1 mice) with *Gata2*^{het} mice (provided by Stuart Orkin) or with *Gata2*$^{+/L359V}$ knockin mice (provided by Sai-Juan Chen). (See detailed description of the mouse model in the *Online Supplementary Methods*.) The studies were approved by the institutional animal care and use committee (1149/18/ANIM).

Immunophenotyping

Bone marrow cells were washed in 2% FBS in PBS and re-suspended in 100 μL staining media (STM) containing fluorochrome conjugated antibodies for 30 minutes. Following staining, cells were washed, re-suspended to a final volume of 100 μL STM, and analyzed with a Gallios 3 laser/10 color flow cytometer (Beckman Coulter, Brea, CA, USA). Leukemia panels are detailed in the *Online Supplementary Methods*.

Histopathology

Femurs and spleens were fixed in 4% neutral buffered formalin, paraffin-embedded, and stained with hematoxylin and eosin using standard protocols.

Methylcellulose re-plating assays

E14.5 fetal liver (FL) cells were harvested and forced through a 70 μm cell strainer into 2% fetal calf serum in PBS at 4°C. Lineage negative cell enrichment was performed using MACS magnetic columns (MACS Miltenyi Biotec, Bergisch Gladbach, Germany). $2x10^4$ cells were plated in methylcellulose supplemented with IL6, IL3, and SCF (MethoCult GF M3534, Stem Cell Technologies, Vancouver, Canada) in duplicates. After seven days, colonies (>50 cells) were counted and re-suspended, and cells were counted and re-plated in the same manner until colonies no longer formed. Three independent experiments were performed, each with 2-3 FL from each genotype.

10x RNA sequencing

A BM-derived single-cell suspension was prepared from each mouse femur, diluted to a concentration of aproximately 1,000 cells/μL, and loaded into the 10x chromium microfluidic system, aiming for 5,000 single cells/sample. An RNA-seq library was prepared for each sample according to the manufacturer's protocol. Final libraries were sequenced using the Nextseq 75 cycles high output kit (Illumina) for a coverage of 50,000 reads/cell. Single cell RNA-seq data analysis is detailed in the *Online Supplementary Methods*. Raw data are available on the Gene Expression Omnibus (GEO) (accession n. GSE143308).

Transmission electron microscopy

Cells were sliced, fixed and mounted on carbon-coated Formvar grids. (Details of the protocol are available in the *Online Supplementary Methods*.) Samples were then stained with uranyl acetate and lead citrate, and examined under a Jeol 1400 Plus transmission electron microscope (Jeol, Tokyo, Japan). Images were captured using SIS Megaview III and the iTEM imaging platform (Olympus, Tokyo, Japan). All mice and human measurements, and calculations in electron microscopy captures were performed using the Fiji open source platform for biological image analysis. Analysis of patients' BM was approved by the institutional review board committee of Rabin Medical Center (approval n. 0840-18-RMC).

Oxygen consumption analysis

Oxygen consumption rates (OCR) were measured using the Seahorse XF96 analyzer (Agilent Technologies, Santa Clara, CA, USA). Cells were treated and cultured with XF assay medium in a Seahorse XF96 cell culture plate (30 μL) before being transferred to the Seahorse XF96 analyzer, as detailed in the *Online Supplementary Methods*.

RNAseq

Total RNA was extracted and purified using the TRIzol™ Plus RNA purification kit (Invitrogen, Carlsbad, CA, USA). Library preparation, sequencing data and expression analysis are all detailed in the *Online Supplementary Methods*.

Results

Gata2 heterozygosity accelerates leukemia in transgenic *ERG* mice

We crossed mice transgenic to human *ERG* (Tg*ERG*; previously shown to develop AML[18,20]) with *Gata2*^{het} mice. There was a significant reduction in time to leukemia and time to survival (log rank Mantel-Cox test, $P<0.0001$) in Tg*ERG/Gata2*^{het} compound mice, compared with Tg*ERG* littermates with a *Gata2*^{WT} background (Figure 1A). To examine the reproducibility of the model, we then crossed a *Gata2*$^{+/L359V}$ knockin mice (provided by Sai-Juan Chen) with Tg*ERG* mice. GATA2 L359V had previously been identified in chronic myeloid leukemia.[22] As with Tg*ERG/Gata2*^{het}, Tg*ERG/Gata2*$^{+/L359V}$ had an accelerated leukemia and a shorter survival time (*Online Supplementary Figure S1A and B*).

Examination of histopathological sections revealed marked BM infiltration and enlargement of spleens with loss of normal architecture in both Tg*ERG/Gata2*^{het} and Tg*ERG/Gata2*^{wt} leukemic mice (*Online Supplementary Figure S1C*). Leukemic cells resided within the CD45^{dim} gate, and was made up of lineage negative; CD150^{high}; cKit$^{low\text{-}pos}$; Sca1^{neg} cells consistent with mega-erythroid progenitors (MEP) (Figure 1B and C).[23] Similar findings were documented within the *Gata2*$^{+/L359V}$ progeny (*Online Supplementary Figure S1D*). Taken together, the accelerated leukemogenesis on the loss of a *Gata2* allele confirms its role as a tumor suppressor.

Transition of hematopoietic stem cell to proliferating progenitor cell in Tg*ERG/Gata2*^{het} pre-leukemic cells

Having established the earlier leukemia development in Tg*ERG* mice on the background of *Gata2* mutation, we were interested in deciphering the pre-leukemic phenotype. We further analyzed differentiation markers on Tg*ERG/Gata2*^{het} and Tg*ERG/Gata2*^{wt} HSPC, isolated from 4-6-week non-leukemic BM. We used two panels to distinguish between stem cells and early progenitor cells: the first included CD150 and CD48 (Slam molecules), and the second included cKit (CD117) and Sca1.[24] Flow cytometry analysis revealed a significantly higher CD48^{pos} /CD48^{neg} ratio within the CD150^{+} population of Tg*ERG/Gata2*^{het} cells (Figure 2A and B). CD48 is an early marker of non-quiescence[25] suggesting increased non-stem progenitors in Tg*ERG/Gata2*^{het} mice. There was a lower fraction of Lin^{-} Sca1^{+}cKit^{+} cells in the Tg*ERG/Gata2*^{het} HSPC compartment consistent with a greater transition from stem to progenitor cells (Figure 2A and C).

We then checked whether associated morphological features can be detected to distinguish Tg*ERG/Gata2*^{het} from Tg*ERG/Gata2*^{wt} HSPC. BM of four pre-leukemic siblings and two leukemic mice were harvested. Hematopoietic lineage negative (lin-) progenitor cells were selected using magnetic beads and subjected to transmission electron microscopy (TEM). A significant decrease in nuclear to cytoplasmic ratio (NCR) was found in Tg*ERG/Gata2*^{het} cells compared with Tg*ERG/Gata2*^{wt} ($P<0.0001$) (Figure 2D). Decreasing NCR during hematopoiesis typically accompanies the gradual transition of pluripotency to lineage commitment and differentiation,[26] and is, therefore, consistent with the dominance of progenitor cells of the Tg*ERG/Gata2*^{het} HSPC compartment.

Early progenitor cells have a greater proliferative capacity than quiescent hematopoietic stem cells.[26] Therefore, we next examined the proliferative potential of Tg*ERG/Gata2*^{het} pre-leukemic HSPC. A clear advantage in colony formation capacity in re-plating methylcellulose assays was observed in Tg*ERG/Gata2*^{het} fetal liver HSPC compared with their counterparts (one-way ANOVA, $P<0.05$) (Figure 3A). We then studied pre-leukemic HSPC derived from BM of age-matched 4-7-week-old mice. Cell trace proliferation assay demonstrated a significantly higher proliferation index of Tg*ERG/Gata2*het HSPC compared to Tg*ERG/Gata2*^{wt} (Figure 3B).

To further identify pre-leukemic HSPC sub-populations in Tg*ERG/Gata2*^{het}, we conducted 10x single cell RNA se-

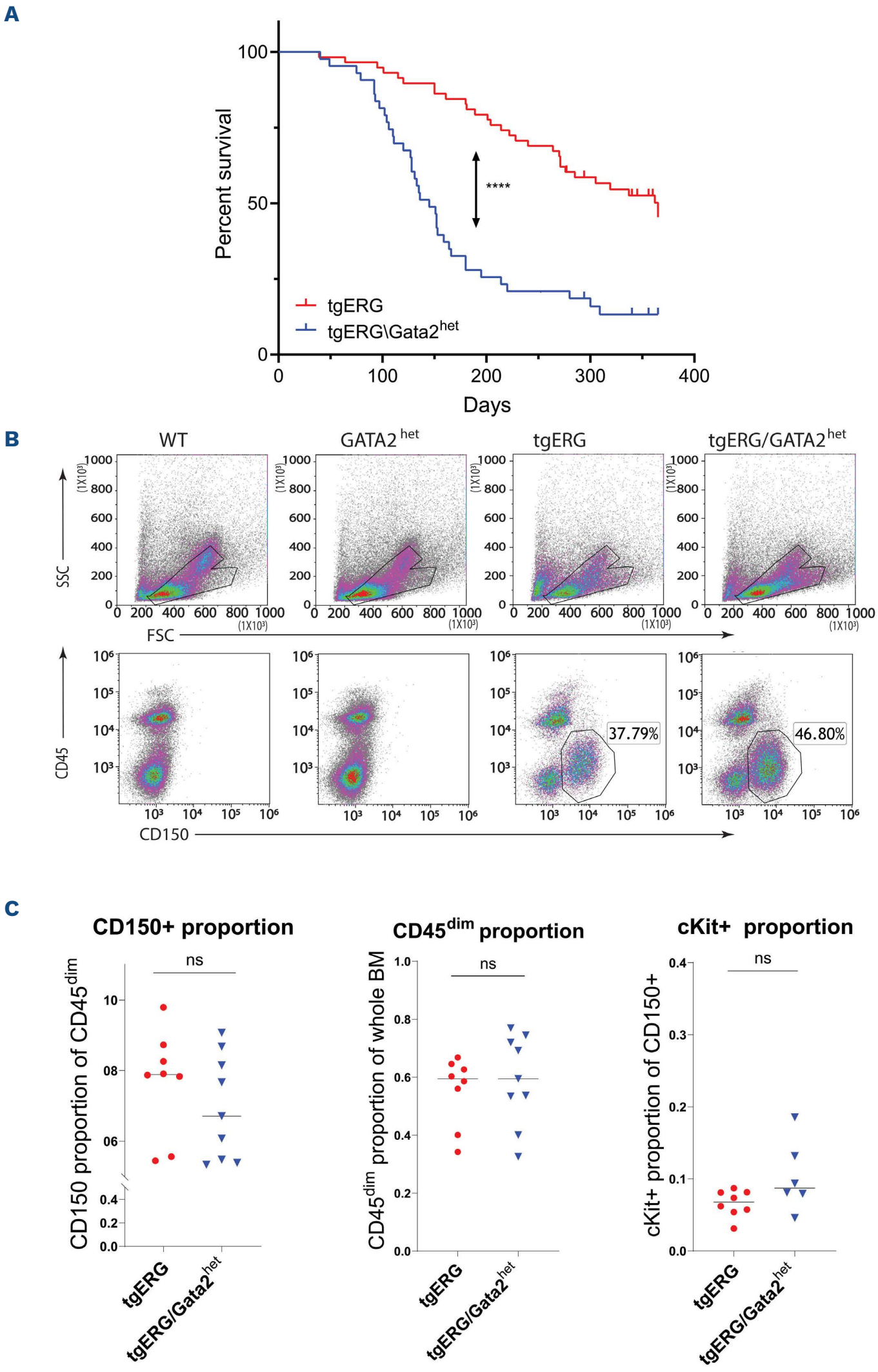

Figure 1. Accelerated leukemia and reduced survival in *Gata2*-haploinsufficient Tg*ERG* mice. (A) Survival curve showing reduced survival (log rank Mantel-Cox test, $^{****}P<0.0001$) in Tg*ERG/Gata2*^{het} (blue: n=43) mice compared to Tg*ERG/Gata2*^{wt} (herein Tg*ERG*, red: n=59) littermates. (B) Flow cytometry plot depicting immune phenotyping of Lin (-) leukemia cells. (Top) Cell scatter. (Bottom) Lin (-) hematopoietic stem and progenitor cells residing in a CD45^{dim} gate, expressing CD150^{high} and cKit$^{low/+}$. Leukemic population is circled. (C) Dot plots of CD45^{dim}, CD150, and cKit showing no differences in proportions of expressed membranal markers between the two leukemias (lines represent mean values; $P<0.05$, Student *t* test). BM: bone marrow; ns: not significant.

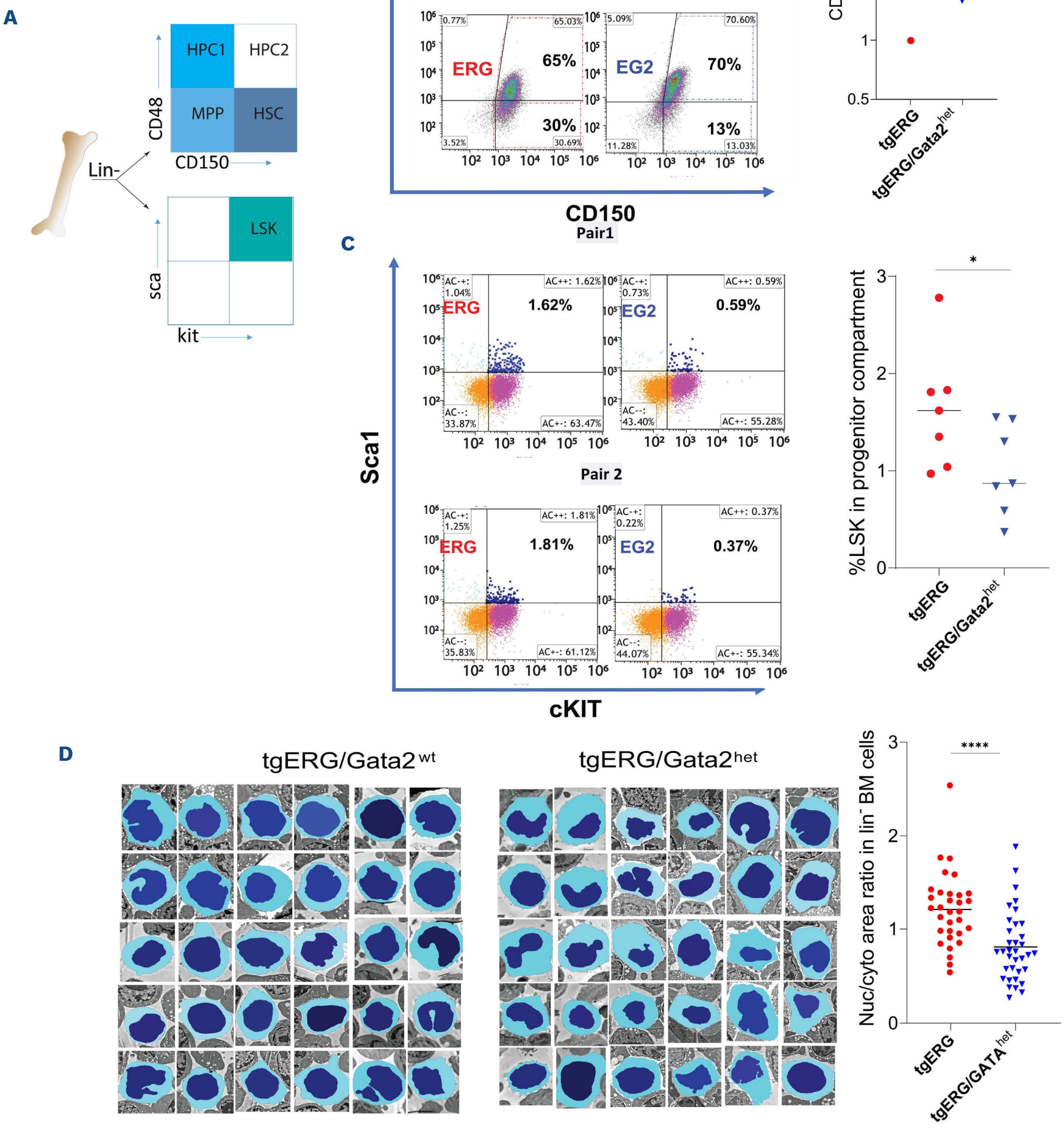

Continued on following page.

Figure 2. Progenitor expansion within Tg*ERG/Gata2*^{het} pre-leukemic hematopoietic stem and progenitor cell compartment. (A) Different stages of progenitors by CD150 and CD48 (slam1, slam2, respectively) combined expression and classical LSK differentiation. Lin- cells were immunophenotyped for progenitor compartments according to SLAM (B) and classical LSK (C) markers. (B) (Left) Representative flow cytometry graphs demonstrating CD48 and CD150 gating approach. (Right) Dot graph summarizing six experiments (n=6; Student *t* test, **P*<0.05). (C) (Left) Representative cytometry plots of two experiments. (Right) Dot graph depicting comparison of LSK proportions (n=7; Student *t* test, **P*<0.05). (D) Transmission electron microscopy images were used to calculate nuclear to cytoplasmic (Nuc/cyto) ratio of leukemic and pre-leukemic cells. (Left) Demarcation of cytoplasm (light blue) and nuclei (dark blue). Cells were derived from two pre-leukemic mice, and one leukemic mouse for either Tg*ERG* (left grid) or Tg*ERG/Gata2*^{het} (right grid). 1:12,000 magnification scale, calibrated by Fiji tool (1 μm=124 pixel). (Right) A decreased nuclear to cytoplasmic ratio was found in Tg*ERG/Gata2*^{het} cells (Student *t* test, *****P*<0.0001). HPC: hematopoietic progenitor cells; HS: hematopoietic stem cells; MPP: multipotential progenitors; BM: bone marrow; ERG: Tg*ERG/Gata2*^{wt}; EG2: Tg*ERG/Gata2*^{het}.

quencing analysis on stem and progenitor cells derived from BM of 4-week-old mice littermates representing the entire genotypic repertoire (*WT*, *Gata2*^{het}, Tg*ERG/Gata2*^{wt}, Tg*ERG/Gata2*^{het}). Tg*ERG/Gata2*^{het} cells harbored a discrete expression pattern, clustering distinctively apart from Tg*ERG/Gata2*^{wt} cells, and from the remaining two control groups (Figure 3C, left). Consistent with the role of ERG and GATA2 in megakaryocytic and erythroid development,[3] a functional annotation map, corresponding to expressed key lineage markers, showed that Early erythroid and Mid erythroid were the main lineage modules to contribute to the distinctive Tg*ERG/Gata2*^{het} expression profile (Figure 3C, right, and *Online Supplementary Figure S2A*). K-means clustering within groups yielded a cluster of differentially expressed genes, up-regulated in the Tg*ERG/Gata2*^{het} sample (*Online Supplementary Figure S2B*). This gene set corresponded to cell proliferation and cell division GO terms. For example, Tg*ERG/Gata2*^{het} cells within the erythroid cluster displayed higher expression of Ki67 proliferation marker as well as the mitotic genes Cenpe and Cenpf (Figure 3D and *Online Supplementary Figure S2C*). Taken together, immunophenotypic, functional and single cell genomic analysis demonstrate that loss of the *WTGata2* allele gave Tg*ERG* pre-leukemic cells an enhanced proliferative and self-renewing hematopoietic progenitor phenotype.

A mitochondrial phenotype in *Gata2* mutated mouse and human hematopoietic cells

To identify potential mechanistic leads that could link *GATA2* loss to the HSPC developmental and proliferative phenotypes, we conducted bulk RNA sequencing experiments in pre-leukemic and leukemic cells. Gene set enrichment analysis (GSEA)[27] showed enrichment of oxidative phosphorylation and mitochondrial metabolism in Tg*ERG/Gata2*^{het}. This signature was consistently found in fetal liver, in pre-leukemia BM, as well as in leukemic cells (Figure 4A and *Online Supplementary Figure S3*). Importantly, oxidative phosphorylation is also a leading gene set expression signature in Tg*ERG/Gata2*$^{+/L359V}$ leukemic cells (*Online Supplementary Figure S4A*) and in a *Gata2*$^{+/L359V}$ mouse model.[28] To clarify whether the metabolic signature observed in Tg*ERG/Gata2*^{het} mice is relevant in humans, we subsequently analyzed expression profiles of AML patients who harbor chromosome 3q26 inversion Inv(3q26)/t(3;3), causing activation of the EVI1 oncogene.[29,30] Intriguingly, oxidative phosphorylation was among the highest ranked pathways to be enriched in *Evi1/GATA2*^{MUT} patients (Figure 4B). Moreover, top ranked gene sets in a *ERG/Gata2*^{het} mouse model and *Evi1/GATA2*^{MUT} (GSEA, Hallmark cluster) shared common modules, including MYC, and mTOR signaling (*Online Supplementary Figure S4B*). The common expression signatures seen in our mouse models and the human leukemias suggest that these models are of a general significance to oncogenic driven AML on the background of GATA2 insufficiency status.

To test the functional significance of the mitochondrial gene expression signature, we conducted a metabolic analysis. HSPC from BM of three pairs of pre-leukemic Tg*ERG/Gata2*^{het} and Tg*ERG/Gata2*^{wt} mouse siblings were analyzed (Seahorse XF96 analyzer). Basal oxygen consumption rate (OCR) was significantly higher in Tg*ERG/Gata2*^{het} HSPC (Figure 4C and *Online Supplementary Figure S5*), and a trend toward higher adenosine triphosphate (ATP) productivity was also found (*Online Supplementary Figure S5*). Interestingly, proton leak was significantly higher in Tg*ERG/Gata2*^{het} cells (*Online Supplementary Figure S5*). The proton leak represents ATP-dissociated influx of H+ ions into the mitochondria and can reflect mitochondrial damage.[31]

To estimate cellular mitochondrial content, we calculated mtDNA to nuclear DNA (nDNA) copy number ratio using ND1 and r16s as mitochondrial genes and HK2 as a nuclear gene (Figure 4D, left). Both ND1/HK2 and r16s/HK2 ratios were significantly higher in Tg*ERG/Gata2*^{het} cells (Figure 4D, middle and right). Together these findings suggest Tg*ERG/Gata2*^{het} HSPC harbor both enhanced oxidative metabolism and mitochondrial abundancy in line with their RNA expression signature.

Disrupted mitochondria in Tg*ERG/Gata2*^{het} hematopoietic progenitors

We investigated whether Tg*ERG/Gata2*^{het} cells undergo mitochondrial morphological alteration. Lin- HSPC of 4-week-old pre-leukemic, and two leukemic, age- and sex-matched Tg*ERG/Gata2*^{wt} and Tg*ERG/Gata2*^{het} mice were analyzed by TEM. Cell captures revealed prominent morphological alterations in Tg*ERG/Gata2*^{het} mitochondria

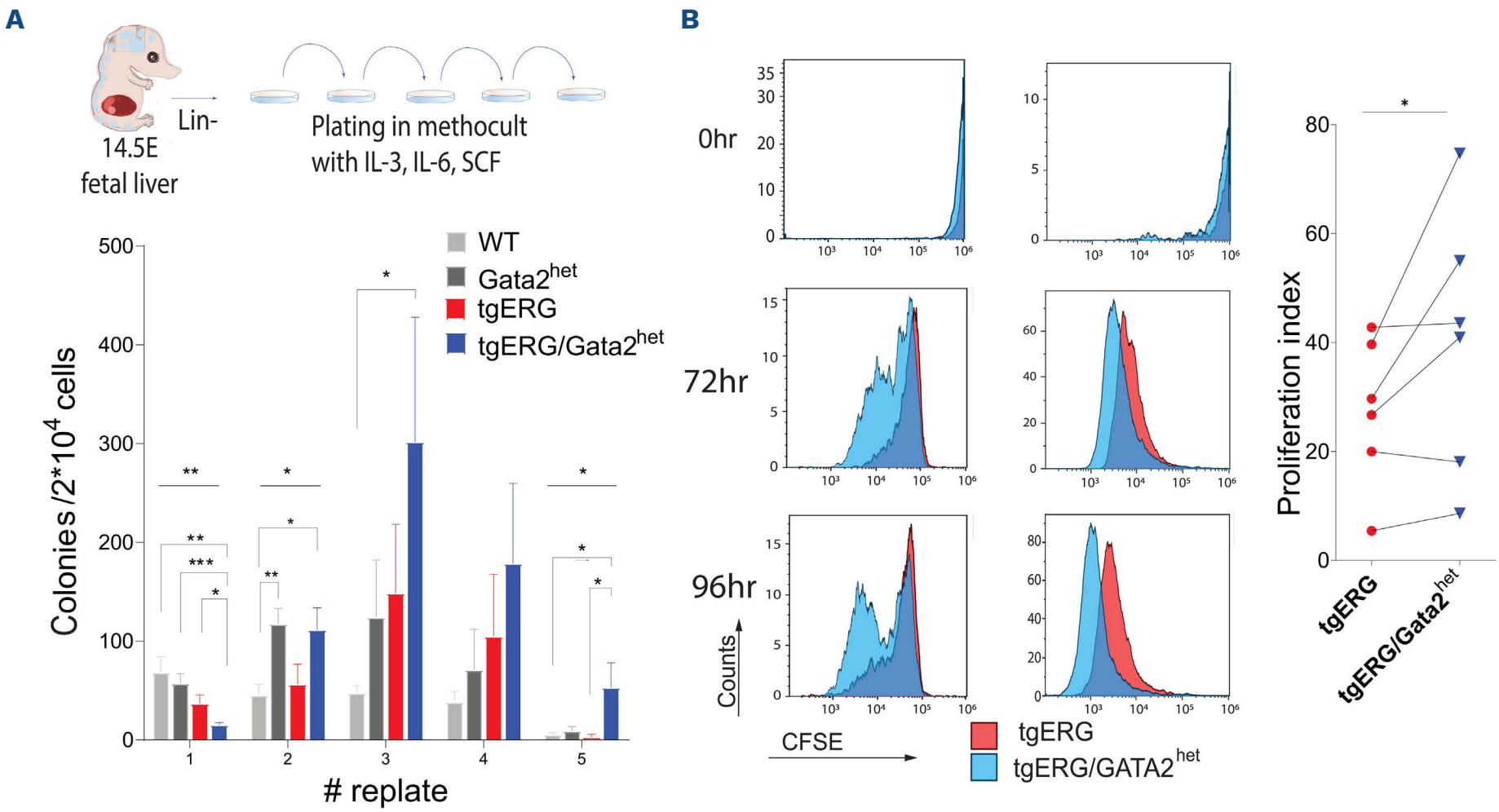

Continued on following page.

Figure 3. Proliferative phenotype in Tg*ERG/Gata2*^{het} pre-leukemia progenitor cells. (A) Enhanced proliferation and re-plating capacity of Tg*ERG/Gata2*^{het} fetal liver hematopoietic stem and progenitor cells (HSPC). (Top) Replanting scheme. (Bottom) Bar graph of 3 independent re-plating assays of E14.5 fetal livers (n=6-8 / genotypic group; oneway ANOVA and unpaired Student *t* test: **P*<0.05, ***P*<0.01, ****P*<0.0001). (B) Tg*ERG/Gata2*^{het} bone marrow HSPC have a higher proliferation index in CFSE assay. (Left) Representative histograms of two CFSE dilutional courses. Tg*ERG/Gata2*^{wt} and Tg*ERG/Gata2*^{het} at 0, 72, and 96 hours (hr) from staining. (Right) Six independent experiments (paired Student *t* test, **P*<0.05). (C) Two-dimensional projection plot of Metacell model on 10x single cell analysis of pre-leukemic lineage negative progenitors showing (top) Tg*ERG*/Gata2^{het} cells clustered distinctively (green zone) from Tg*ERG/Gata2*^{wt} (red zone), and from *Gata2*^{het} (light blue), and *WT* (purple). Light blue line delineates the area were Tg*ERG/Gata2*^{wt} and Tg*ERG/Gata2*^{het} clustered differentially. (Bottom) Functional annotation plot of Metacells by expression of key lineage markers, depicting Early erythroid (pink) and Mid erythroid (red) modules, are dominantly expressed in both Tg*ERG/Gata2*^{het} and Tg*ERG/Gata2*^{wt} expression profiles shown by projecting the genotype expression map (top) over the lineage expression map (bottom). Differences in expression between Tg*ERG/Gata2*^{wt} and Tg*ERG/Gata2*^{het} mostly occur in Early and Mid erythroid. An additional line provides an approximate separation of Early from Mid erythroid program zones. (D) Ki67, Cenpf and Cenpe (mitosis-related genes) expression projections on metacell plot are illustrated together with the global expression scheme of Tg*ERG/Gata2*^{het} (upper left). The genes are highly expressed in Tg*ERG/Gata2*^{het} territory. Dark blue: high expression; yellow-white: low expression; ERG: Tg*ERG*: Tg*ERG/Gata2*^{wt}; ERG_GATA2:Tg*ERG/Gata2*^{het}; GATA2: *Gata2*^{het}.

showing swelling, circular contour, and co-localization in clusters. Conversely, Tg*ERG/Gata2*^{wt} mitochondria were small, thread-shaped, and spread evenly within the cytoplasm (Figure 5A). In addition, the ratio of cumulative mitochondrial area to the cytoplasm of a cell was significantly higher in Tg*ERG/Gata2*^{het} (*P*<0.0001) (Figure 5B), indicating a higher mitochondrial content (Figure 5B), consistent with the genomic quantification (Figure 4D).

Ultra-structural characterization of the mitochondrial morphology revealed ill-defined disrupted cristae in Tg*ERG/Gata2*^{het}. Some mitochondria were enclosed in a double membraned vacuole, suggesting mitophagy. Conversely, Tg*ERG/Gata2*^{wt} mitochondria were elongated and convoluted, with clear electron-dense crista (Figure 5C, left). Analysis of individual mitochondrion features documented a larger mean area of an individual Tg*ERG*/Gata2^{het} mitochondrion. (Student *t* test, *P*<0.0001) (Figure 5C, middle). In addition, the aspect ratio (obtained by dividing the mitochondrial longest axis by the shortest axis), ranging from elongated to round, was significantly lower in Tg*ERG*/Gata2^{het} mitochondria (Student *t* test, *P*<0.0001) (Figure 5C, right). This feature can be related to differences in mitochondrial dynamics, such as fission preference over fusion, associated with cell division[32] or to increased degradation due to mitochondrial damage. The unique mitochondrial morphology detected in Tg*ERG/Gata2*^{het} HSPC is consistent with the metabolic phenotype. Interestingly, TEM analysis of cells from *GATA2* heterozygous mice did not show the same aberrant mitochondrial morphological phenotype as that seen in the Tg*ERG/Gata2*^{het} mouse cells (*Online Supplementary Figure S7*), although gene expression analysis of progenitor cells from *GATA2*^{het} demonstrated an upregulation in oxidative phosphorylation gene expression (*Online Supplementary Figure S8*), in agreement with the minimal hematologic phenotype observed in *GATA2*^{het} mice.

Abnormal mitochondria in hematopoietic progenitors from bone marrow of children with germline GATA2$^{+/R396W}$ mutation

To test whether humans with germline mutated *GATA2* present mitochondrial aberrancy, we examined CD34+ BM cells derived from two siblings of one family harboring the GATA2$^{+/R396W}$ mutation (Figure 6A). A 13-year-old male was diagnosed with a germline GATA2 R396W mutation after presenting with aplastic anemia. A genetic analysis of the family revealed the mutation to be transmitted from the asymptomatic father to three of his children: the proband 13-year-old symptomatic son, a 15-year-old asymptomatic daughter, and a 7-year-old asymptomatic son. A fourth male sibling (11 years old) did not inherit the mutation (Figure 6B).

Complete blood count of the proband patient at presentation demonstrated pancytopenia with severe neutropenia (200 cells/μL), monocytopenia (10 cells/μL), and thrombocytopenia (24*10^3/μL). Both asymptomatic carrier siblings displayed normal blood counts with normal cellular indexes. Cytogenetic and somatic gene panel sequencing analysis[7] was normal for both proband and carriers. BM biopsy of the proband revealed remarkable hypocellularity (20% of normal) with myelodysplastic changes. Importantly, although her blood count was normal, the sister's BM demonstrated minimal myelodysplastic changes. No BM examinations were performed for the youngest male carrier or the father.

More than 25 CD34+ BM cells from the patient and the carrier sister were captured using TEM (FEI Tecnai SPIRIT, FEI, Eidhoven, The Netherlands), analyzed, and compared with CD34+ BM cells of a healthy donor. There was a clear difference in general cell morphology: normal control CD34+ cells had a homogenous cytoplasm, and well-defined, electron dense mitochondria, while the mitochondria of GATA2$^{+/R396W}$ cells of both sister and the patient had an abnormal appearance with fragmentation, polymorphism, and disrupted cristae (Figure 6C and D). While quantitative analysis of the mitochondrial morphometrics of the patient's CD34+ cells was difficult to establish due to pronounced cellular disruption and vacuolization, we found the sister's cells to have a significantly decreased mitochondrial aspect ratio, as in the Tg*ERG/Gata2*^{het} mice, but average size of the mitochondria was also reduced,

A

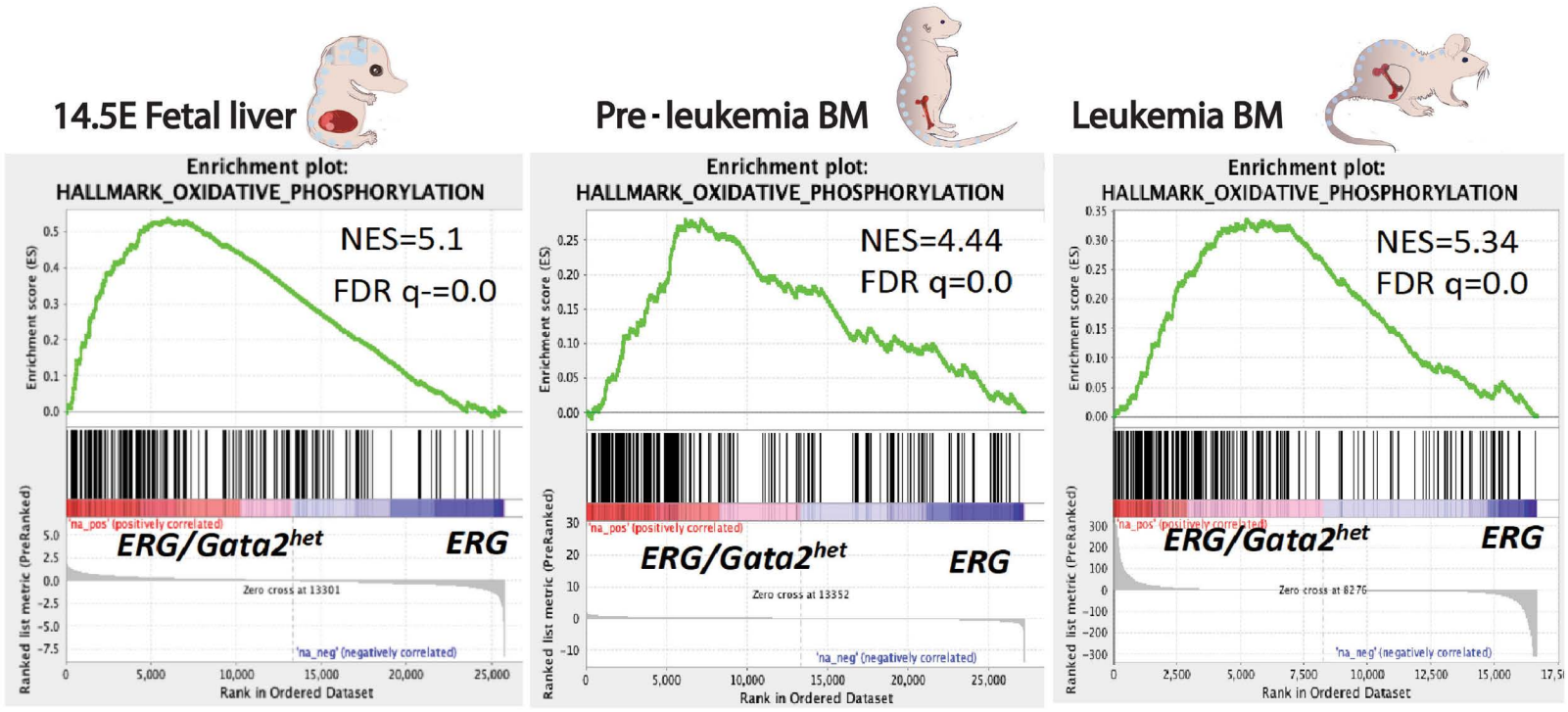
14.5E Fetal liver
Pre-leukemia BM
Leukemia BM
Enrichment plot:
HALLMARK_OXIDATIVE_PHOSPHORYLATION
NES=5.1
FDR q-=0.0
NES=4.44
FDR q=0.0
NES=5.34
FDR q=0.0
Enrichment score (ES)
'na_pos' (positively correlated)
ERG/Gata2het
ERG
Zero cross at 13301
Zero cross at 13352
Zero cross at 8276
'na_neg' (negatively correlated)
Ranked list metric (PreRanked)
Rank in Ordered Dataset

B

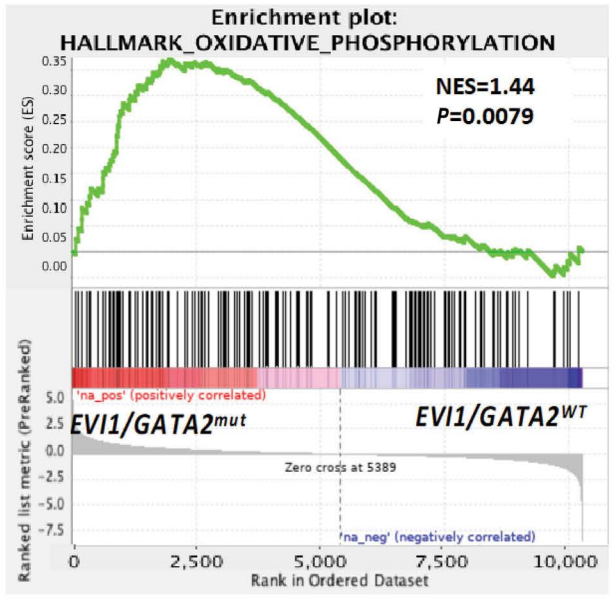
Human leukemia BM
Enrichment plot:
HALLMARK_OXIDATIVE_PHOSPHORYLATION
NES=1.44
P=0.0079
Enrichment score (ES)
'na_pos' (positively correlated)
EVI1/GATA2mut
EVI1/GATA2WT
Zero cross at 5389
'na_neg' (negatively correlated)
Ranked list metric (PreRanked)
Rank in Ordered Dataset

C

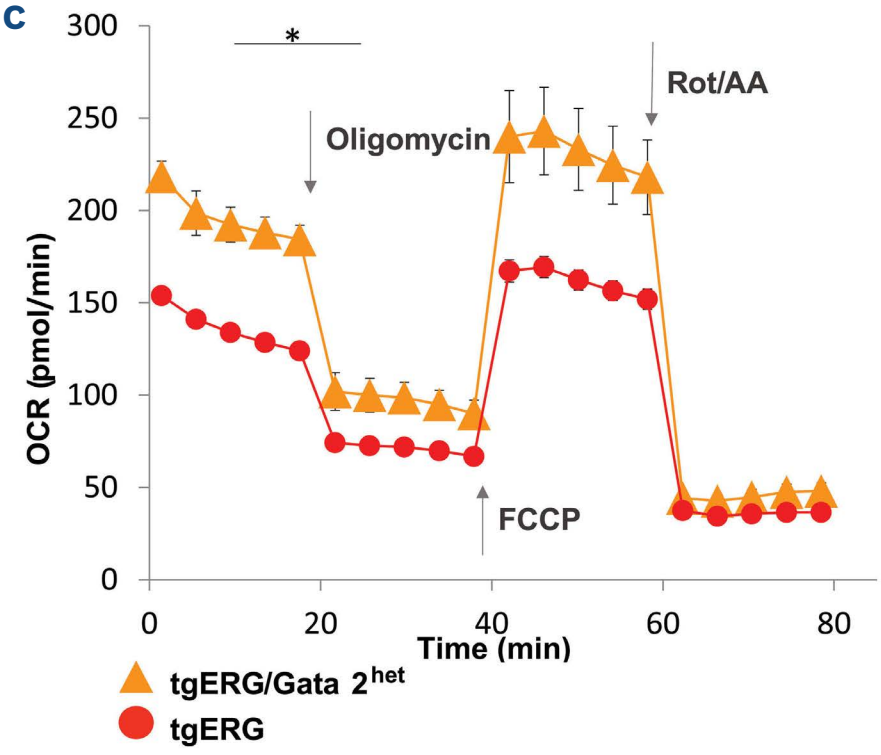
OCR (pmol/min)
Time (min)
Oligomycin
Rot/AA
FCCP
tgERG/Gata 2het
tgERG

D

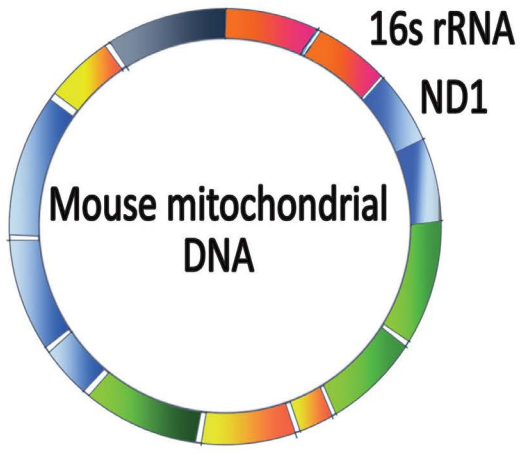
16s rRNA
ND1
Mouse mitochondrial DNA

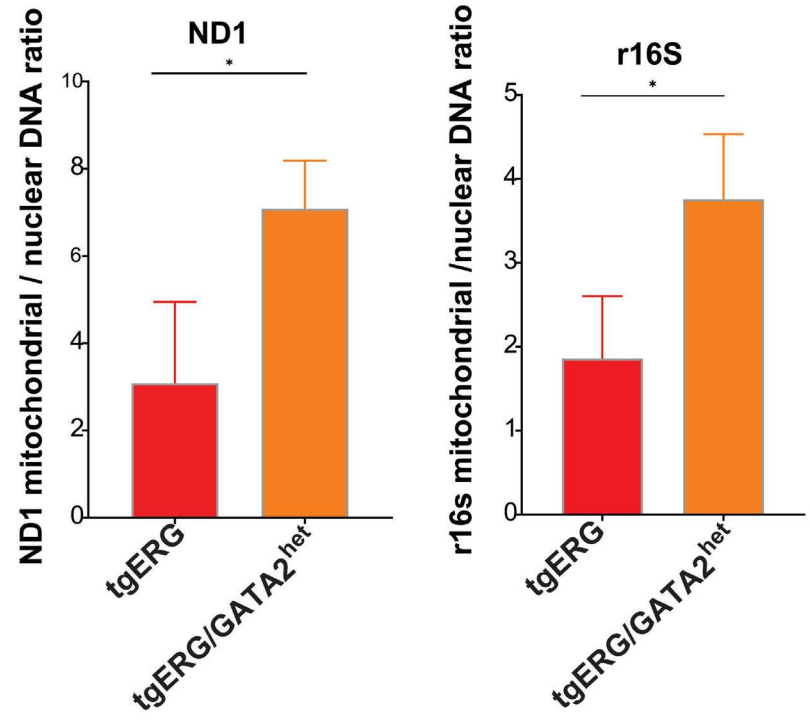
ND1
r16S
ND1 mitochondrial / nuclear DNA ratio
r16s mitochondrial /nuclear DNA ratio
tgERG
tgERG/GATA2het

Figure 4. Enhanced oxidative phosphorylation in *GATA2* mutated leukemias. (A) Gene Set Enrichment Analysis (GSEA) plots depicting oxidative phosphorylation pathway enrichment in Tg*ERG/Gata2*^{het} RNAseq expression profiles compared with Tg*ERG/Gata2*^{wt}. (B) GSEA plot showing oxidative phosphorylation signature is enriched in human Inv(3)/GATA2-mutated acute myeloid leukemia cell expression profiles. (C) Basal oxygen consumption rate (OCR) is significantly higher in Tg*ERG/Gata2*^{het} hematopoietic stem and progenitor pre-leukemia cells (HSPC); SeaHorse XF assay. One of 3 independent experiments. Arrows show time of intervention. min: minutes. Student *t* test, **P*<0.05. (D) (Left) Mouse mitochondrial DNA with ND1 and r16s genes marked. (Right) qPCR quantitation of mitochondrial to nuclear DNA ratio calculated using ND1 and r16s. Tg*ERG/Gata2*^{het} HSPC harbor a higher ratio of mitochondrial/nuclear DNA copy number. N=3-4. HK2: nuclear reference gene. Student *t* test, **P*<0.05. ERG: Tg*ERG*: Tg*ERG/Gata2*^{wt}; ERG/GATA2^{het}: Tg*ERG/Gata2*^{het}.

reflecting the ongoing fragmentation (Figure 6E). Compared with normal BM, GATA2$^{+/R396W}$ cells of both the patient and the sister showed a decrease in nuclear cytoplasmic ratio (*P*<0.0001) (*Online Supplementary Figure S9*), similar to that observed in Tg*ERG/Gata2*^{het} mouse progenitors. Therefore, disrupted mitochondria and reduced NCR characterize human GATA2 deficiency HSPC, as observed in the Tg*ERG/Gata2*^{het} mouse.

Discussion

Disruptive germline mutations in *GATA2* represent a significant risk of developing MDS/AML. Current research has described a variety of effects of GATA2 loss on increasing the virulence of myeloid and erythroid leukemias.[12,15-17] Here we investigated the effect of *GATA2* haploinsufficiency on the pre-leukemic phenotype. The tumor suppressive function of GATA2 was uncovered by accelerated ERG-driven leukemias in mice with germline *Gata2* mutations. We identified enhanced transition of pre-leukemic HSC into proliferating early progenitors. These pre-leukemic progenitors had increased mitochondrial oxidative phosphorylation and increased mitochondrial content with prominent mitochondrial structural aberrations. Strikingly, abnormal mitochondria were detected also in pre-leukemic BM of patients with germline *GATA2* mutation, including an asymptomatic carrier.

Several attempts have been made to unravel the tumor suppressive effect of GATA2 in mouse models by crossing *Gata2* mutated mice with mice expressing oncogenic leukemic mutations. Some of these models displayed either complex phenotype or no malignant transformation,[33] while others accelerated the acute leukemic occurrence[16] or altered the leukemic phenotype.[17] For example, Liu *at al.*[15] reported enhanced leukemic stem cell phenotype in leukemias arising in a Cbfb-MYH11 knockin/Gata2 heterozygous mouse; however, paradoxically, latency time to leukemia was longer. Thus, oncogenes themselves may enable the tumor suppressive effect of GATA2.

Here we exploited Tg*ERG* mice to uncover the GATA2 tumor suppressive effect in the pre-leukemic phenotype. ERG is a hematopoietic transcription factor regulating stemness in both normal and leukemic stem cells.[34-39] Indeed, ERG co-regulate HSPC together with GATA2 as part of a heptad of transcription factors.[39] ERG, GATA2 and TAL1, three of the Heptad's factors, act in a loop to regulate erythropoiesis.[3] Strikingly, ERG has recently been shown to be the main driver of leukemias characterized by haploinsufficiency of GATA2 and EVI-1 overexpression.[21] These EVI-1 AML are highly similar to our mouse model. Interestingly, ERG and GATA2 also co-operate in other types of cancers, particularly prostate cancer.[40] Thus, our mouse model is highly relevant, as ERG is a likely oncogene-mediating leukemia progression of GATA2 germline haploinsuffiency.

The main observation in our study is the presence of marked mitochondrial abnormalities associated with increased expression of oxidative phosphorylation genes and elevated oxygen consumption rates in pre-leukemic Gata2 deficient cells. Interestingly, enhanced expression of genes mediating oxidative phosphorylation were also reported by Yamamoto *et al.*[16] in murine AML driven by EVi-1 and Gata2 deficiency. Similar to ERG, Evi-1 is also a hematopoietic stem cell transcription factor and an upstream activator of GATA2.[41] Here we show that this mitochondrial gene expression signature exists also in human EVI-1 leukemias with somatic GATA2 mutations. Similarly, activation of oxidative phosphorylation was demonstrated in progression of myeloproliferative neoplasms following loss of LK1/STK11.[42] However, here we demonstrate, for the first time in both the mouse model and in children carrying a GATA2 mutation, that the mitochondrial aberrations occur very early, long before progression to frank MDS or leukemia.

These findings may be of general relevance to AML/MDS, as prior reports suggested mitochondrial dysfunction and impaired elimination of defective mitochondria (e.g., mitophagy) in MDS/AML.[43] An increased number of mitochondria-containing autophagosomes and enlarged abnormal mitochondria were also shown in early erythroblasts of MDS patients.[44,45] The described mitochondria phenotype of structural double membrane vacuoles in conjugation with abnormal mitochondrial structure (Figure 5) in *GATA2*^{het} (Figure 6) and Tg*ERG/Gata2*^{het} may suggest mitophagy involvement in both the pre-leukemia state generated by *GATA2*^{het} and in the leukemia. MDS patients were reported to have mitophagy involvement in progression to leukemia. Houwerzijl *et al.* showed that erythroid precursors from high-risk MDS patients have lower mi-

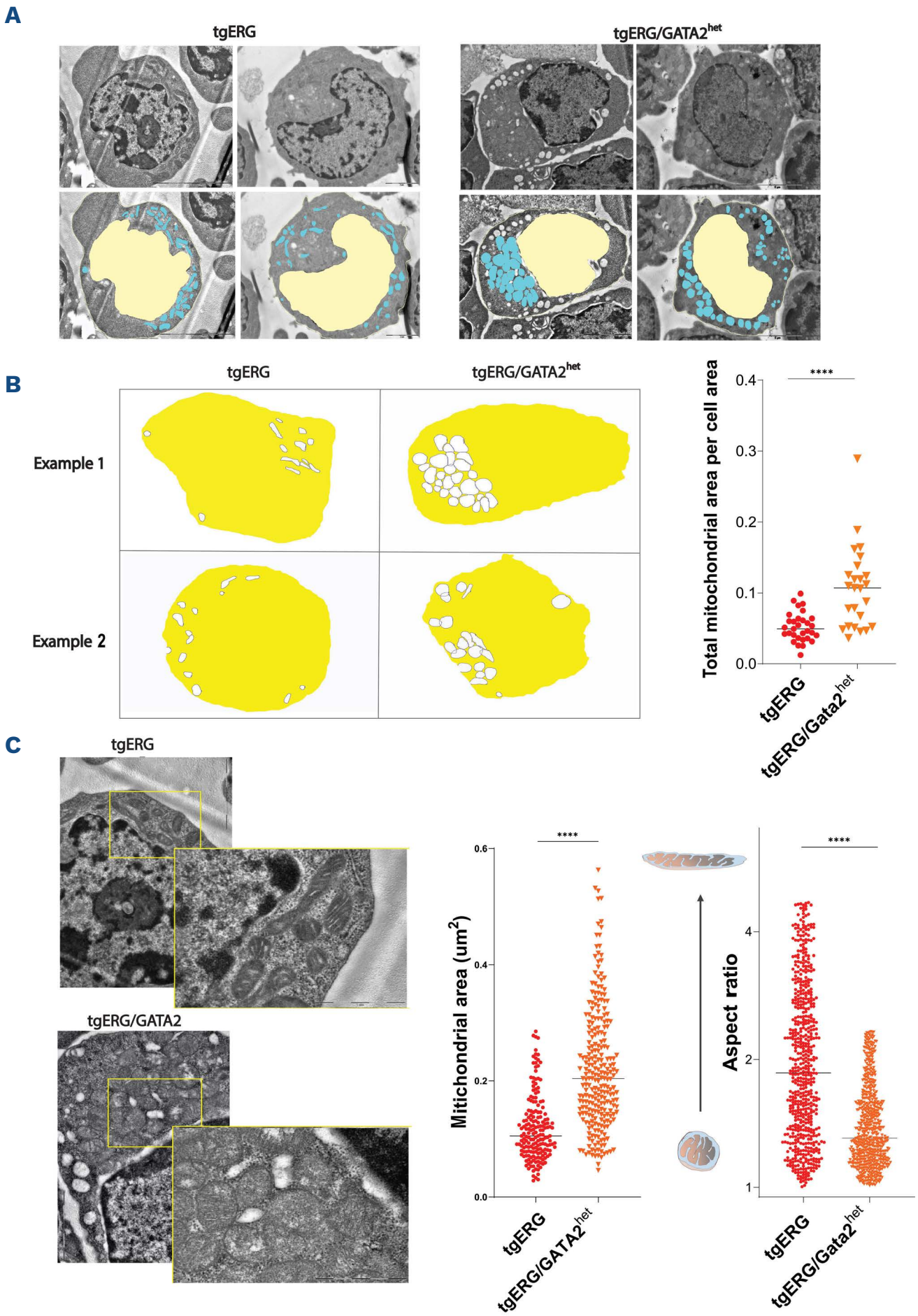

Figure 5. Mitochondrial structural aberrations in Tg*ERG/Gata2*^{het} pre-leukemic hematopoietic progenitors. (A) Tg*ERG/Gata2*^{het} hematopoietic lineage negative progenitors exhibit mitochondrial disruptions, as shown in transmission electron microscopy which captures imaging both in pre-leukemia and leukemia cells. (Left) Tg*ERG/Gata2*^{wt} hematopoietic stem and progenitor cell (HSPC) mitochondria are spread within cytoplasm. (Right) Tg*ERG/Gata2*^{het} mitochondria are swollen, rounded, and tend to group in clusters. (Top) Unprocessed capture. (Bottom) ImageJ processed view. Light-blue: mitochondria; beige: nuclei. Scale 1:12,000. (B) Total mitochondrial surface per cell is increased in Tg*ERG/Gata2*^{het} hematopoietic progenitors. Representative illustration by ImageJ (left), and dot bar graph (right). N=25-31 cells per genotype; unpaired Student *t* test, ****P<0.0001. (C) (Left) Mitochondria ultra structures of Tg*ERG/Gata2*^{wt} progenitors (Tg*ERG*) are elongated, torturous, and display electron dense, clearly defined cristae (vertical frame). Tg*ERG/Gata2*^{het} progenitors display spherical, swollen mitochondria and distorted, blurred cristae (horizontal frame). Scale 1: 20,000 ; 1:50,000, respectively; yellow quadrangles show magnified view of mitochondrial structure. (Center) Dot plot showing mean surface area of an individual mitochondrion is higher in Tg*ERG/Gata2*^{het} progenitors. Unpaired Student *t* test, ****P<0.0001. (Right) Dot plot showing mitochondrial aspect ratio, representing longest to shortest axis ratio, is lower in Tg*ERG/Gata2*^{het} . Unpaired Student *t* test, P<0.0001. Note the spherical contour rather than a thread shape. (Calculated by Fiji NIH program.[50]); Tg*ERG*: Tg*ERG/Gata2*^{wt}.

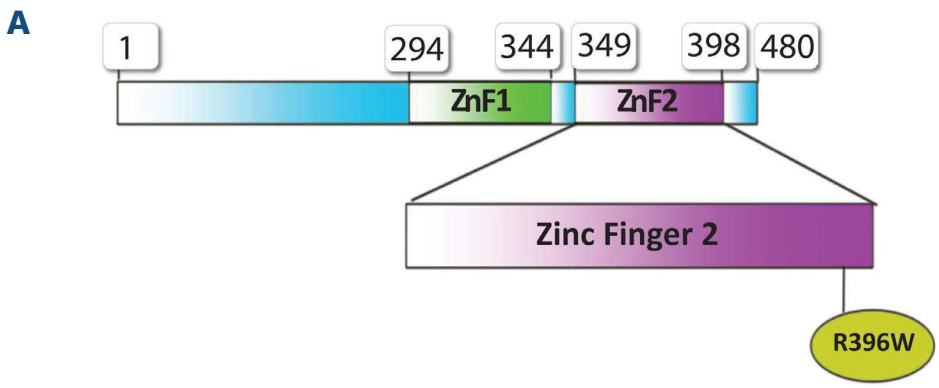

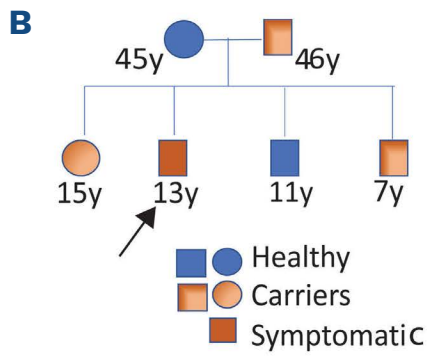

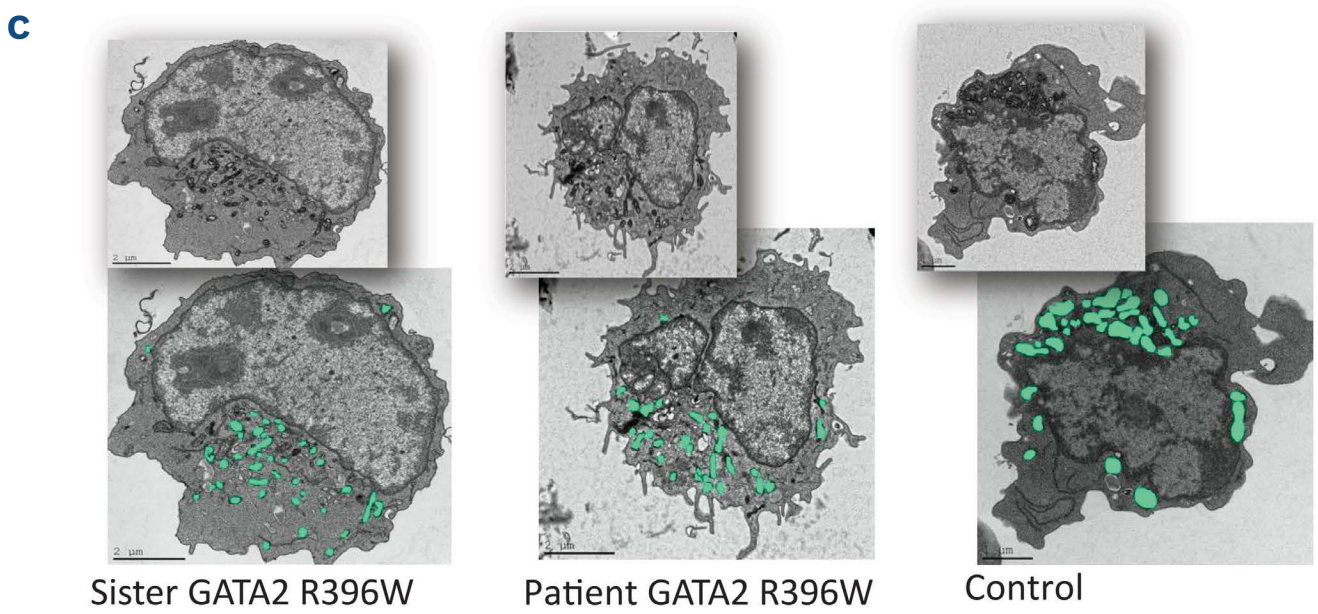

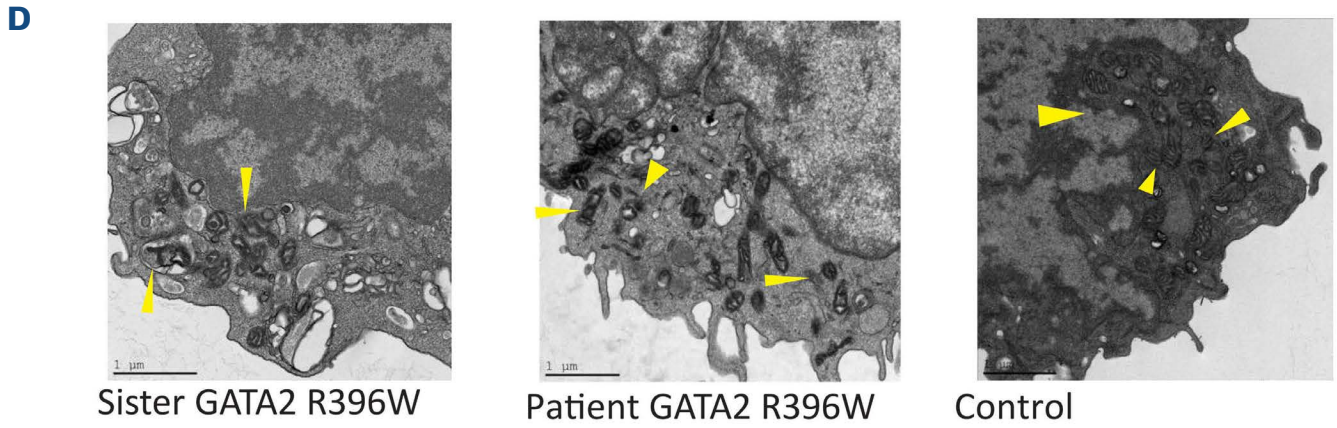

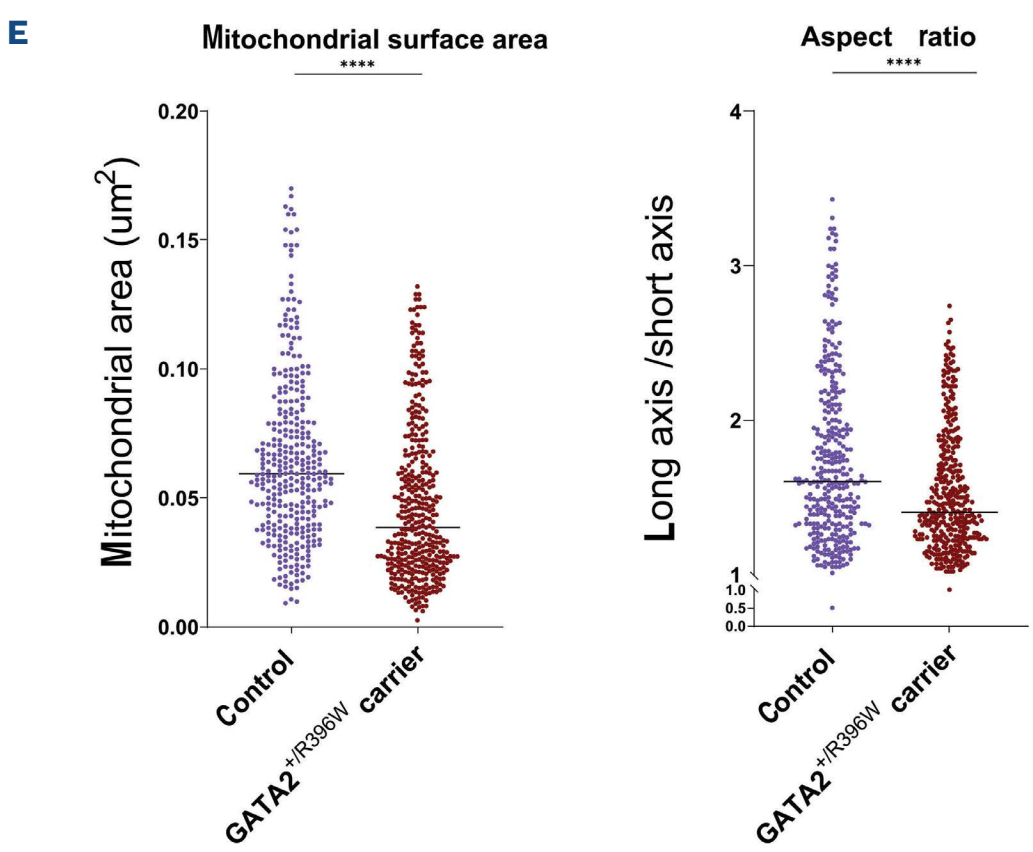

Continued on following page.

Figure 6. Mitochondrial aberrations in human GATA2$^{+/R396W}$ mutated hematopoietic progenitors. (A) Schematic illustration of the GATA2 germline R396W substitution mutation switching Arginine to Tryptophan. (B) Family pedigree of the 13-year-old GATA2+/R396W patient (arrow) diagnosed and treated in our hospital. Circle: female; quadrangle; male; y: age in years. (C) Transmission electron microscopy captures of CD34+ bone marrow (BM) cells show fragmented mitochondria (top quadrangles: original capture) designated by pseudo-color light green (large quadrangles). Fragmentation is shown in carrier sister and the patient (left and middle, respectively) compared to normal sized and normal contour mitochondria of donor CD34+ BM cells (right). (Scale 1:4,800 to 1:6,800, Fiji NIH program.[50]) (D) Mitochondria ultrastructure. Fragmentation and disruption of cristae in carrier and sister (left and middle captures, respectively), and organized well-defined and electron-dense cristae in mitochondria of the control cells (right capture) (FEI Tecnai SPIRIT, Eindhoven, The Netherlands). Scale 1:6,800-1:9,300. (E) Mean surface area of an individual mitochondrion is lower (left) in GATA2$^{+/R396W}$ carrier (sister) CD34+ hematopoietic stem and progenitor cells compared with normal control (unpaired Student *t* test, ****P<0.0001). Mitochondrial aspect ratio (right), representing longest to shortest axis ratio, is lower in GATA2$^{+/R396W}$ carrier, which reflects fragmented formation instead of thread shape. (Calculated by Fiji NIH program.[50]] Unpaired Student *t* test, ****P<0.0001.

tophagy levels compared with low-risk MDS patients. In addition, an MDS mouse model that was generated by deletion of the autophagy protein Atg7, (Vav-Atg7$^{-/-}$) resulted in a decreased LSK CD150^{+}CD48^{-} HSC compartment (which is the population that we describe) and upregulation of the myeloid leukemia marker CD47.[46]

Analysis of pre-leukemic cells by single cell RNA sequencing revealed that erythroid committed progenitors are the main population that contribute to the differences in expression patterns between Tg*ERG/Gata2*^{wt} and Tg*ERG/Gata2*^{het}. Our observation is similar to recently published findings by Nerlov *et al.*[17] There, the authors show that *Gata2* mutation synergized with CEBPa double mutation to generate a permissive erythroid chromatin state that promotes leukemogenesis of bilineage acute erythroid /myeloid leukemia. The expansion of highly proliferating erythroid precursors in the Tg*ERG/Gata2*^{het} mice was also associated with monocytopenia (*Online Supplementary Figure S6*), which is often observed in human carriers of germline GATA2 mutations.[47]

The transition to highly proliferating hematopoietic progenitors was also confirmed by immunophenotyping, *in vitro* self-renewal proliferation assays, TEM analysis of nuclear to cytoplasmic ratio, and single cell gene expression analysis. Interestingly, our observation of expanded progenitor compartment (cKit+ lin- and sca1-) and reduced fraction of KLS cells in BM of Tg*ERG/Gata2*^{het} pre-leukemic mice, is also supported by Nerlov *et al.*; in their study, GATA2 loss led to expanded progenitors but not an expanded KLS compartment.[17] Our observations are reinforced by developmental studies of *Gata2* heterozygous mice that provide qualitative and quantitative evidence that diminished hematopoietic stem cells are accompanied by expansion of hematopoietic progenitors.[1,13] Thus, GATA2 haploinsufficiency may create a premature aging phenotype of HSPC characterized by increased transition to progenitors coupled with increased susceptibility to oncogenic transformation.

The transition from quiescence to proliferative pre-leukemic progenitors may also partially explain the mitochondrial phenotype in Tg*ERG/Gata2*^{het}. This transition generates a steep increase in energetic demands, and hence, oxidative phosphorylation preference over glycolysis, mitochondrial fission/ fragmentation, and a flux of reactive oxygen species.[48] The loss of GATA2 as a stem cell gate keeper may result in the transition from quiescence into a proliferative state associated with increased mitochondrial mass and activity. If unrestricted cycling is ongoing, the cellular scavenging machinery may fail to sufficiently neutralize genotoxic molecules. Abnormal mitochondrial dynamics may have a genuine effect on GATA2-deficiency leukemogenic evolvement, a vulnerability that could be exploited therapeutically to prevent and treat these leukemias. While several drugs have been suggested to lower leukemia mitochondrial activity (reviewed by Egan *et al.*[49]), replacing BM transplantation by chronic drug therapy suppressing the pre-leukemic phenotype is a major challenge and represents one of the leading “unmet needs” in the management of cancer predisposition syndrome. The question remains as to whether a pharmacological approach can alter its course.

Disclosures

No conflicts of interest to disclose.

Contributions

SI, YB and AR designed the research; AR, YB, IG, EK, HF and IA carried out the research; S-JC, RD, SG, RM-L, SL-Z, ND, VH, IA, JY, OS-S, Q-HH, YT and EG contributed new reagents and/or analytic tools; AR, AG, IG, YB, EG, RD, IA, RM-L, TNR, S-JC, Q-HH, YT and SI analyzed the data; AR, YB and SI wrote the paper.

Acknowledgments

We thank Professor Atan Gross for his invaluable advice regarding mitochondrial metabolism and analysis, Jonatan Barel for RNAseq analysis, and to Hadas Keren-Shaul for 10X RNA sequencing services. We are indebted to Itzhak Ben Moshe and Erez Shtosel for mouse care, and past and present members of Shai Izraeli's research group for fruitful discussion and advice. This research was carried out in partial fulfilment of the requirements for

Avigail Rein's PhD degree at the Sackler Faculty of Medicine, Tel Aviv University, Israel.

Funding

This study was supported by the Israel Science Foundation and the National Science Foundation China (to SI and S-JC), the Israeli Ministry of Science and DKFZ (to SI and SG), the Waxman Cancer Research Foundation (to SI), the Ministry of Health (to SI), the Larger Than Life Foundation (to SI and AR), Hans Neufeld Stiftung (to SI) and ICCF (to SI), The Dotan Center of Hematological Malignancies, Tel Aviv University (to SI), the ICRF Professorship grant (to SI) and the Nevzlin Foundation (to SI).

Data-sharing statement

Raw data are available in GEO through accession GSE143238 at: https://www.ncbi.nlm.nih.gov/geo/query/acc.cgi?acc=GSE143238 and accession GSE143308 at: https://www.ncbi.nlm.nih.gov/geo/query/acc.cgi?acc=GSE143308

References

1. Rodrigues NP, Janzen V, Forkert R, et al. Haploinsufficiency of GATA-2 perturbs adult hematopoietic stem-cell homeostasis. Blood. 2005;106(2):477-484.
2. Tsai FY, Keller G, Kuo FC, et al. An early haematopoietic defect in mice lacking the transcription factor GATA-2. Nature. 1994;371(6494):221-226.
3. Thoms JAI, Truong P, Subramanian S, et al. Disruption of a GATA2-TAL1-ERG regulatory circuit promotes erythroid transition in healthy and leukemic stem cells. Blood. 2021;138(16):1441-1455.
4. Menendez-Gonzalez JB, Vukovic M, Abdelfattah A, et al. Gata2 as a crucial regulator of stem cells in adult hematopoiesis and acute myeloid leukemia. Stem Cell Reports. 2019;13(2):291-306.
5. Chaytor L, Simcock M, Nakjang S, et al. The pioneering role of GATA2 in androgen receptor variant regulation is controlled by bromodomain and extraterminal proteins in castrate-resistant prostate cancer. Mol Cancer Res. 2019;17(6):1264-1278.
6. Kennedy JA, Ebert BL. Clinical implications of genetic mutations in myelodysplastic syndrome. J Clin Oncol. 2017;35(9):968-974.
7. Noy-Lotan S, Krasnov T, Dgany O, et al. Incorporation of somatic panels for the detection of haematopoietic transformation in children and young adults with leukaemia predisposition syndromes and with acquired cytopenias. Br J Haematol. 2021;193(3):570-580.
8. Donadieu J, Lamant M, Fieschi C, et al. Natural history of GATA2 deficiency in a survey of 79 French and Belgian patients. Haematologica. 2018;103(8):1278-1287.
9. Al Seraihi AF, Rio-Machin A, Tawana K, et al. GATA2 monoallelic expression underlies reduced penetrance in inherited GATA2-mutated MDS/AML. Leukemia. 2018;32(11):2502-2507.
10. Wlodarski MW, Hirabayashi S, Pastor V, et al. Prevalence, clinical characteristics, and prognosis of GATA2-related myelodysplastic syndromes in children and adolescents. Blood. 2016;127(11):1387-1397; quiz 1518.
11. Churpek JE, Bresnick EH. Transcription factor mutations as a cause of familial myeloid neoplasms. J Clin Invest. 2019;129(2):476-488.
12. Sahoo SS, Kozyra EJ, Wlodarski MW. Germline predisposition in myeloid neoplasms: unique genetic and clinical features of GATA2 deficiency and SAMD9/SAMD9L syndromes. Best Pract Res Clin Haematol. 2020;33(3):101197.
13. de Pater E, Kaimakis P, Vink CS, et al. Gata2 is required for HSC generation and survival. J Exp Med. 2013;210(13):2843-2850.
14. Dzierzak E, Bigas A. Blood development: hematopoietic stem cell dependence and independence. Cell Stem Cell. 2018;22(5):639-651.
15. Saida S, Zhen T, Kim E, et al. Gata2 deficiency delays leukemogenesis while contributing to aggressive leukemia phenotype in Cbfb-MYH11 knockin mice. Leukemia. 2020;34(3):759-770.
16. Katayama S, Suzuki M, Yamaoka A, et al. GATA2 haploinsufficiency accelerates EVI1-driven leukemogenesis. Blood. 2017;130(7):908-919.
17. Di Genua C, Valletta S, Buono M, et al. C/EBPalpha and GATA-2 mutations induce bilineage acute erythroid leukemia through transformation of a neomorphic neutrophil-erythroid progenitor. Cancer Cell. 2020;37(5):690-704.e8.
18. Goldberg L, Tijssen MR, Birger Y, et al. Genome-scale expression and transcription factor binding profiles reveal therapeutic targets in transgenic ERG myeloid leukemia. Blood. 2013;122(15):2694-2703.
19. Taoudi S, Bee T, Hilton A, et al. ERG dependence distinguishes developmental control of hematopoietic stem cell maintenance from hematopoietic specification. Genes Dev. 2011;25(3):251-262.
20. Birger Y, Goldberg L, Chlon TM, et al. Perturbation of fetal hematopoiesis in a mouse model of Down syndrome's transient myeloproliferative disorder. Blood. 2013;122(6):988-998.
21. Schmoellerl J, Barbosa IAM, Minnich M, et al. EVI1 drives leukemogenesis through aberrant ERG activation. Blood. 2023;141(5):453-466.
22. Zhang SJ, Ma LY, Huang QH, et al. Gain-of-function mutation of GATA-2 in acute myeloid transformation of chronic myeloid leukemia. Proc Natl Acad Sci U S A. 2008;105(6):2076-2081.
23. Pronk CJ, Rossi DJ, Mansson R, et al. Elucidation of the phenotypic, functional, and molecular topography of a myeloerythroid progenitor cell hierarchy. Cell Stem Cell. 2007;1(4):428-442.
24. Boles KS, Nakajima H, Colonna M, et al. Molecular characterization of a novel human natural killer cell receptor homologous to mouse 2B4. Tissue Antigens. 1999;54(1):27-34.
25. Oguro H, Ding L, Morrison SJ. SLAM family markers resolve functionally distinct subpopulations of hematopoietic stem cells and multipotent progenitors. Cell Stem Cell. 2013;13(1):102-116.
26. Passegue E, Wagers AJ, Giuriato S, Anderson WC, Weissman IL. Global analysis of proliferation and cell cycle gene expression in the regulation of hematopoietic stem and progenitor cell fates. J Exp Med. 2005;202(11):1599-1611.
27. Subramanian A, Tamayo P, Mootha VK, et al. Gene set enrichment analysis: a knowledge-based approach for interpreting genome-wide expression profiles. Proc Natl Acad Sci U S A. 2005;102(43):15545-15550.
28. Fu YK, Tan Y, Wu B, et al. Gata2-L359V impairs primitive and

definitive hematopoiesis and blocks cell differentiation in murine chronic myelogenous leukemia model. Cell Death Dis. 2021;12(6):568.
29. Groschel S, Sanders MA, Hoogenboezem R, et al. A single oncogenic enhancer rearrangement causes concomitant EVI1 and GATA2 deregulation in leukemia. Cell. 2014;157(2):369-381.
30. Yamazaki H, Suzuki M, Otsuki A, et al. A remote GATA2 hematopoietic enhancer drives leukemogenesis in inv(3)(q21;q26) by activating EVI1 expression. Cancer Cell. 2014;25(4):415-427.
31. Divakaruni AS, Paradyse A, Ferrick DA, Murphy AN, Jastroch M. Analysis and interpretation of microplate-based oxygen consumption and pH data. Methods Enzymol. 2014;547:309-354.
32. Khacho M, Clark A, Svoboda DS, et al. Mitochondrial dynamics impacts stem cell identity and fate decisions by regulating a nuclear transcriptional program. Cell Stem Cell. 2016;19(2):232-247.
33. Shimizu R, Yamamoto M. Quantitative and qualitative impairments in GATA2 and myeloid neoplasms. IUBMB Life. 2020;72(1):142-150.
34. Loughran SJ, Kruse EA, Hacking DF, et al. The transcription factor Erg is essential for definitive hematopoiesis and the function of adult hematopoietic stem cells. Nat Immunol. 2008;9(7):810-819.
35. Lacadie SA, Zon LI. The ERGonomics of hematopoietic stem cell self-renewal. Genes Dev. 2011;25(4):289-293.
36. Knudsen KJ, Rehn M, Hasemann MS, et al. ERG promotes the maintenance of hematopoietic stem cells by restricting their differentiation. Genes Dev. 2015;29(18):1915-1929.
37. Salek-Ardakani S, Smooha G, de Boer J, et al. ERG is a megakaryocytic oncogene. Cancer Res. 2009;69(11):4665-4673.
38. Yassin M, Aqaqe N, Yassin AA, et al. A novel method for detecting the cellular stemness state in normal and leukemic human hematopoietic cells can predict disease outcome and drug sensitivity. Leukemia. 2019;33(8):2061-2077.
39. Diffner E, Beck D, Gudgin E, et al. Activity of a heptad of transcription factors is associated with stem cell programs and clinical outcome in acute myeloid leukemia. Blood. 2013;121(12):2289-2300.
40. Buscheck F, Zub M, Heumann A, et al. The independent prognostic impact of the GATA2 pioneering factor is restricted to ERG-negative prostate cancer. Tumour Biol. 2019;41(7):1010428318824815.
41. Sato T, Goyama S, Nitta E, et al. Evi-1 promotes para-aortic splanchnopleural hematopoiesis through up-regulation of GATA-2 and repression of TGF-b signaling. Cancer Sci. 2008;99(7):1407-1413.
42. Marinaccio C, Suraneni P, Celik H, et al. LKB1/STK11 is a tumor suppressor in the progression of myeloproliferative neoplasms. Cancer Discov. 2021;11(6):1398-1410.
43. Joshi A, Kundu M. Mitophagy in hematopoietic stem cells: the case for exploration. Autophagy. 2013;9(11):1737-1749.
44. Watson AS, Mortensen M, Simon AK. Autophagy in the pathogenesis of myelodysplastic syndrome and acute myeloid leukemia. Cell Cycle. 2011;10(11):1719-1725.
45. Houwerzijl EJ, Pol HW, Blom NR, van der Want JJ, de Wolf JT, Vellenga E. Erythroid precursors from patients with low-risk myelodysplasia demonstrate ultrastructural features of enhanced autophagy of mitochondria. Leukemia. 2009;23(5):886-891.
46. Mortensen M, Soilleux EJ, Djordjevic G, et al. The autophagy protein Atg7 is essential for hematopoietic stem cell maintenance. J Exp Med. 2011;208(3):455-467.
47. Bigley V, Collin M. Dendritic cell, monocyte, B and NK lymphoid deficiency defines the lost lineages of a new GATA-2 dependent myelodysplastic syndrome. Haematologica. 2011;96(8):1081-1083.
48. Filippi MD, Ghaffari S. Mitochondria in the maintenance of hematopoietic stem cells: new perspectives and opportunities. Blood. 2019;133(18):1943-1952.
49. Egan G, Khan DH, Lee JB, Mirali S, Zhang L, Schimmer AD. Mitochondrial and metabolic pathways regulate nuclear gene expression to control differentiation, stem cell function, and immune response in leukemia. Cancer Discov. 2021;11(5):1052-1066.
50. Valente AJ, Maddalena LA, Robb EL, Moradi F, Stuart JA. A simple ImageJ macro tool for analyzing mitochondrial network morphology in mammalian cell culture. Acta Histochem. 2017;119(3):315-326.